Optimal Hybrid Vehicle Control with Relaxed Speed Constraints

Ziheng Pan, Shaobing Xu, and Huei Peng
University of Michigan
E-mail: zihpan@umich.edu; xushao@umich.edu; hpeng@umich.edu

Reducing fuel consumption is an important design goal for hybrid electric vehicles. Most studies for hybrid electric vehicle control problems assume that the vehicle follow a desired drive cycle exactly. In this paper, we study the control optimization problem with relaxed constraints, i.e., the vehicle has a slack range for either speed or range, which is closer to real-world operations. We study a parallel hybrid vehicle using dynamic programming. Simulation results show that the fuel consumption can reduce by 3%-20% by exploring the new flexibility in relaxed speed or range constraint.

Invited Session Title: Recent Advances on Design and Control of HEVs

1. INTRODUCTION

Hybrid powertrain is an important technology to reduce vehicles' fuel consumptions. With additional electric motor(s), this technology enables additional degree-of-freedom (DOF) to the powertrain system, which allows rooms to optimize the engine operation, e.g., the engine can always run in the high-efficiency area. Its successful implementation on passenger cars has demonstrated the superior benefit on fuel efficiency. As Fig. 1 shows results labeled by US Environmental Protection Agency (EPA), hybrid powertrain can achieve over 100% improvement on fuel economy compared to the conventional technology [1].

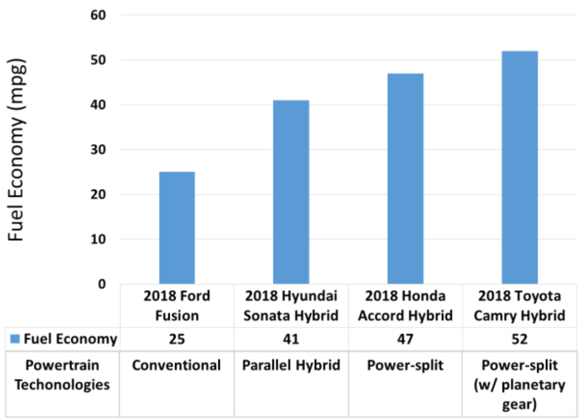

Fig. 1 Fuel Economy Comparisons of Different Hybrid Technologies and Conventional Powertrain [1]

Most previous hybrid electric vehicle (HEV) control studies assume that vehicle follows a desired drive cycles exactly [2-6]. In real world, however, vehicles do not exactly follow the defined drive cycles. In fact, even when testing for vehicle fuel economy, the EPA allows a small range of speed tolerance (±2mph) as shown in Fig. 2, taken from the SAE standard J1711 [7]. This speed tolerance can be exploited to reduce fuel consumption. When considering this "relaxed speed constraint", we call the associated optimal control problems as "relaxed optimization".

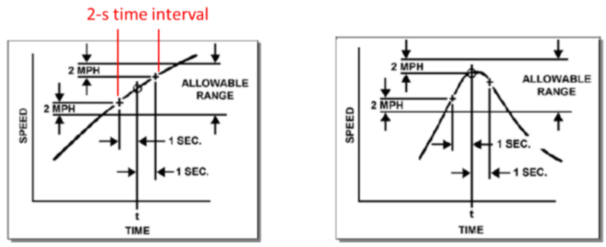

Fig. 2 EPA Defined Tolerance (SAE J1711)

This relaxed optimization can be an important strategy application for connected automated vehicles (CAVs). When managing the traffic fleet, the tailing vehicles do not need to follow the exactly same speed of the leading vehicle. Instead, those vehicles can alter their speeds within acceptable range and achieve additional fuel reduction [8-10].

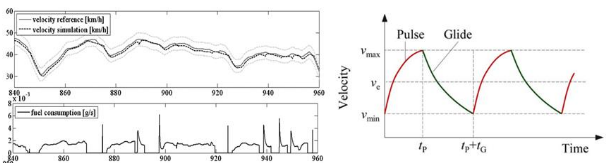

Fig. 3 Bosch SSC (Left) and Pulse-and-Glide (Right)

Several studies [8-15] indicated when such relaxed constrained problem is solved, fuel consumption can reduce by 2-55% for conventional vehicles, compared with the original "rigid", or "non-relaxed problem. For example, the start/stop coasting (SSC) strategy from Bosch [11, 12] allows the test vehicle to more or less follow a desired speed profile, but the speed is allowed to vary within a narrow range, and real-world test results show up to 19% fuel consumption reduction. The pulse-and-glide (PnG) strategy proposed in [10, 13-15] results in up to 55% fuel reduction in cruising scenario. The PnG strategy has been known and used in many super-mileage competition vehicles, but the flip-flop of power could cause concerns for ride quality. Exemplary vehicle speed trajectories are shown in Fig. 3. McDonough's work [8, 9] also indicate that the fuel consumption can be reduced 10-13% in car-following scenario if range and speed constraints are relaxed for the tailing vehicle to vary its speed.

To further improve the fuel efficiency for HEVs, this paper studies and solves the optimal hybrid vehicle control with relaxed speed/range constraints, which is capable of improving fuel economy. Different methods were used to study the benefit of relaxed optimization. Rule-based method was used in the Bosch start-stop coasting for real-life testing [11, 12]; stochastic dynamic programming (SDP) was used in car-following scenario [8, 9]; pseudo-spectral was used to solve the optimal control problem in constant speed cruising scenario [10, 15]. Results from the above methods are either not optimal guaranteed or are hard to apply to general driving scenarios. To fully understand the potential of relaxed optimization for HEVs, we use the dynamic programming (DP) [16] technique to solve the relaxed optimization problem, because it guarantees global optimality and can handle these problems with mixed continuous and discrete controls/states.

The major contribution of this paper is to fully investigate the benefits of the relaxed optimization concept for HEVs by solving the high dimensional non-convex control problem. The remainder of this paper is organized as follows: Section 2 introduces the concept of constraints relaxation; Section 3 presents problem formulation for HEVs relaxed optimization; Section 4 describes the DP procedure to solve the parallel HEV control problem; Section 5 presents the simulation results and analysis; and finally Section 6 summarizes this paper.

2. CONSTRAINTS RELAXATION

This paper focuses on minimizing fuel consumption among various topics of control problems in automotive.

For conventional vehicles with a step-gear automatic transmission, gear position is the only control of the optimization problem when evaluating the vehicle's fuel consumption under defined drive cycles. Engine torque and engine speed are dependent on the gear position, desired vehicle speed and torque. A general problem formulation is shown in Eq. (1), where $\dot{m}_f$ refers to the engine fuel rate, ω_e is the engine speed, T_e refers to the engine torque, and f_e is the function that represents the relationship between $\dot{m}_f$, T_e, and ω_e. Tv_k and v_k represents the vehicle torque and speed at time step k, respectively, and R_{tire} is the tire radius. J is the total cost of fuel consumption.

$$\begin{aligned} \min \quad & J = \sum_{k=0}^{N-1} \dot{m}_f(k) \\ s.t. \quad & T_e = \frac{T_{v_k}}{n_{gear}} \\ & \omega_e = v_k \cdot \frac{1}{R_{tire}} \cdot n_{gear} \\ & \dot{m}_f = f_e(\omega_e, T_e) \end{aligned} \tag{1}$$

For HEVs, they have additional DOFs because electrical components added to the system. The additional electric motor(s) allow engine control flexibility with larger feasible control set. The battery state of charge (SOC) in the hybrid system can be any values within its range (0.3~0.8), and this condition allows the engine changes its torque or/and speed state given a desired vehicle command. Therefore, it can be interpreted that the battery SOC is relaxed constraints to the optimal control problem. A general problem formulation for HEV is shown in Eq. (2), where P_{batt} is the battery power, f_{batt} represents the battery dynamics related to the motor speed ω_m, motor torque T_m, and motor efficiency η_m, $\dot{SOC}$ represents the change rate of SOC, and SOC_{min} and SOC_{max} are the lower and upper limits, respectively.

$$\begin{aligned} \min \quad & J = \sum_{k=0}^{N-1} \dot{m}_f(k) \\ s.t. \quad & \dot{\Omega} = A^{-1} \cdot T \\ & \omega_e = v_k \cdot \frac{1}{R_{tire}} \cdot n_{gear} \\ & \dot{m}_f = f_e(\omega_e, T_e) \\ & s_k = \sum_{i=1}^{k} v_k dt \\ & S\dot{O}C = f_{bat}(P_{bat}) \\ & P_{bat} = \omega_m \cdot T_m \cdot \eta_m \\ & SOC_{\min} \le SOC \le SOC_{\max} \end{aligned} \tag{2}$$

As indicated in Section 1, the vehicle speed of vehicle control problem can be relaxed instead of following the exact speed profile. In this case, the torque output from transmission does not need to deliver exact demanded value at the given speed level. Combining all the relaxation including battery SOC constraint, vehicle speed constraint, and vehicle range constraint, the relaxed optimization for HEV is developed. A general problem formulation is shown in Eq. (3), where v_k and s_k represent vehicle speed and range (or distance between the controlled vehicle and leading vehicle), respectively, and $\underline{v}_k$, $\overline{v}_k$, $\underline{s}_k$, and $\overline{s}_k$ are the lower and upper limits for each state respectively.

$$
\begin{aligned}
\min \quad & J = \sum_{k=0}^{N-1} \dot{m}_f(k) \\
s.t. \quad & \dot{\Omega} = A^{-1} \cdot T \\
& \omega_e = v_k \cdot \frac{1}{R_{tire}} \cdot n_{gear} \\
& \dot{m}_f = f_e(\omega_e, T_e) \\
& s_k = \sum_{i=1}^{k} v_k dt \\
& S\dot{O}C = f_{bat}(P_{bat}) \\
& P_{bat} = \omega_m \cdot T_m \cdot \eta_m \\
& SOC_{\min} \le SOC \le SOC_{\max} \\
& \underline{v}_k \le v_k \le \overline{v}_k, \forall k \\
& \underline{s}_k \le s_k \le \overline{s}_k, \forall k
\end{aligned}
\tag{3}
$$

3. FORMULATION OF HEVS CONTROL WITH RELAXED VEHICLE SPEED

In this paper, a pre-transmission parallel hybrid powertrain for truck application is used for the case study as shown in Fig. 4. The powertrain consists of an internal combustion engine (ICE), an electric motor, and a 6-speed automatic transmission. There is a clutch between the engine and the transmission so that the engine can be disconnected from the powertrain.

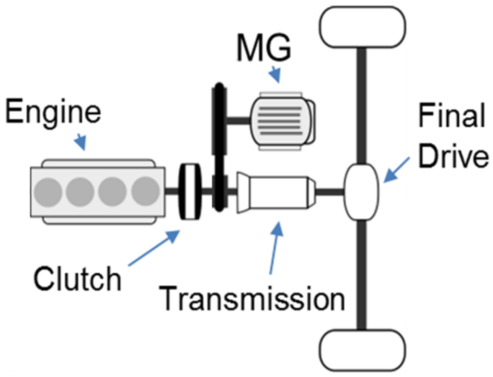

Fig. 4 Schematic of a Pre-Transmission Parallel Hybrid Design

The fuel rate consumed $\dot{m}_f$ is obtained from a look-up table calculated from a Brake Specific Fuel Consumption (BSFC) map, as shown in Fig. 5. Constraints of engine speed ω_e and torque T_e are indicated in the BSFC map and considered throughout the design process.

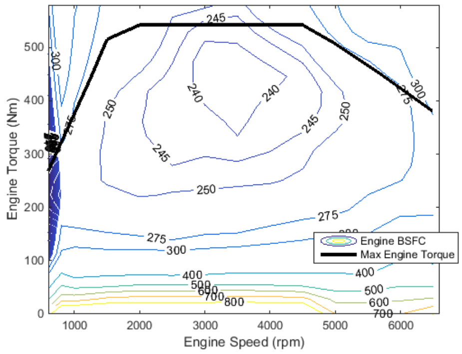

Fig. 5 Engine BSFC Map

Similarly, the efficiency of the electric machine is obtained from the look-up table shown in Fig. 6.

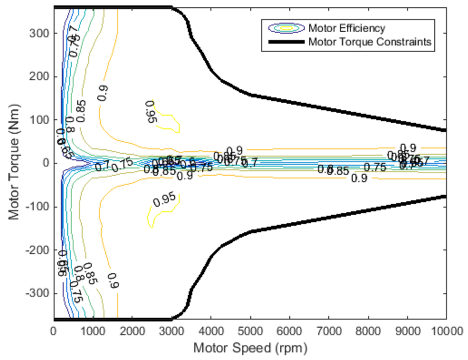

Fig. 6 Motor Efficiency Map

The battery is modeled as a simple open-circuit voltage model with a constant internal resistance. The battery SOC is described in Eq. (4), where V_{oc} is the open-circuit voltage, and R_{batt} is the battery internal resistance.

$$
S\dot{O}C = -\frac{V_{oc} - \sqrt{V_{oc}^{\ 2} - 4 R_{bat} P_{batt}}}{2 \cdot R_{bat}} \tag{4}
$$

The automatic transmission is modeled as a perfect gear model. The relationship of the speed and torque are shown in Eq. (5), together with the vehicle dynamics shown in Eq. (6), where a_v represents the vehicle acceleration, m is the vehicle mass, g is the gravity constant, μ is the resistance coefficient, ρ is the air density, C_d is the drag coefficient, A is the maximum vehicle cross section area, and R_{tire} is the tire radius.

$$
\begin{aligned}
\omega_e &= v_k \cdot n_{gear} \\
T_e &= \frac{T_{v_k}}{n_{gear}}
\end{aligned}
\tag{5}
$$

$$
T_v = \left(mg\mu + \frac{1}{2}\rho C_d A v^2 + m a_v \right) \cdot R_{tire} \tag{6}
$$

Summarizing all the models in Eq. (3) – Eq. (6), the HEV optimal control problem with relaxed speed and range constraints are formulated in Eq. (7).

$$
\begin{aligned}
\min \quad & J=\sum_{k=0}^{N-1}\dot{m}_f(k) \\
s.t. \quad & T_e=\frac{T_{v_k}}{n_{gear}} \\
& \omega_e=v_k\cdot\frac{1}{R_{tire}}\cdot n_{gear} \\
& \dot{m}_f=f_e(\omega_e,T_e) \\
& s_k=\sum_{i=1}^{k}v_k dt \\
& T_v=\left(mg\mu+\frac{1}{2}\rho C_d A v^2+m a_v\right)\cdot R_{tire} \\
& S\dot{O}C=-\frac{V_{oc}-\sqrt{V_{oc}{}^2-4R_{bat}P_{elect}}}{2\cdot R_{bat}} \\
& P_{bat}=\omega_m\cdot T_m\cdot\eta_m \\
& \eta_m=f_m(\omega_m,T_m) \\
& \underline{v}_k\le v_k\le\overline{v}_k,\forall k \\
& \underline{s}_k\le s_k\le\overline{s}_k,\forall k
\end{aligned}
\tag{7}
$$

For the relaxed optimization for parallel hybrid electric vehicle, there are 3 controls (engine torque, motor torque, and transmission gear) and 3 states (SOC, vehicle speed, vehicle range). The problem is nonlinear and non-convex because of the vehicle dynamics and the components' maps. Moreover, the problem has both continuous and discrete controls. In the following section, DP is used to solve this complex problem.

4. DYNAMIC PROGRAMMING

DP is commonly used to solve non-linear non-convex optimal control problems because it is able to guarantee global optimality of results y and it is flexible to handle constraints.

The original problem in Eq. (8) is decomposed into a set of sub-optimization problems for each time step k as shown in Eq. (9), where r_k represents the transitional cost at step k, R_N represents the final cost at step N, and J_k refers to the optimal cost-to-go from step k to the final step N. Then, DP solves these sub-problems backward. Based on the Bellman's principle of optimality, the obtained results are global optimal.

$$\min \quad J=\left(R_N(x_N)+\sum_{k=0}^{N-1}r_k(x_k,u_k)\right) \tag{8}$$

$$J_k(x_k)=\min\left\{r_k(x_k,u_k)+J_{k+1}(x_{k+1})\right\} \tag{9}$$

To implement DP to solve the relaxed optimization formulated in Eq. (7), the problem is decomposed into horizon series of sub-optimization problems. For each stage, all the possible controls with all possible states are combined to calculate transitional fuel cost $\dot{m}_f$ using the system dynamics. This 1st step for transition control is shown in Fig. 7 highlighted in green.

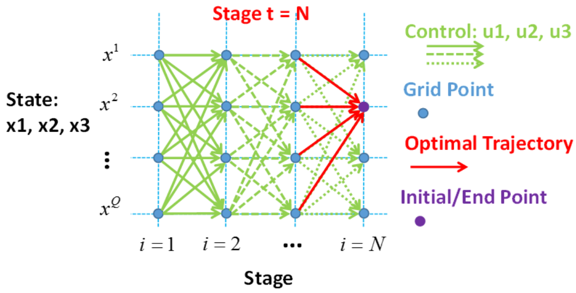

Fig. 7 DP Step 1: Transition Control Cost

At the 2nd step, starting from the end stage, all sub-problems, are optimized backward till the 1st stage is reached. Eq. (10) shows the sub-problem optimization at step k. Based on the principle of optimality, at each stage, the problem is optimal to the end stage. As Fig. 8 shows, when the optimization process reaches the 1st stage, the optimal control from the beginning to the end of the entire control problem is found.

$$J_k(SOC_k)=\min\left\{\dot{m}_{f_k}+J_{k+1}(SOC_{k+1})\right\} \tag{10}$$

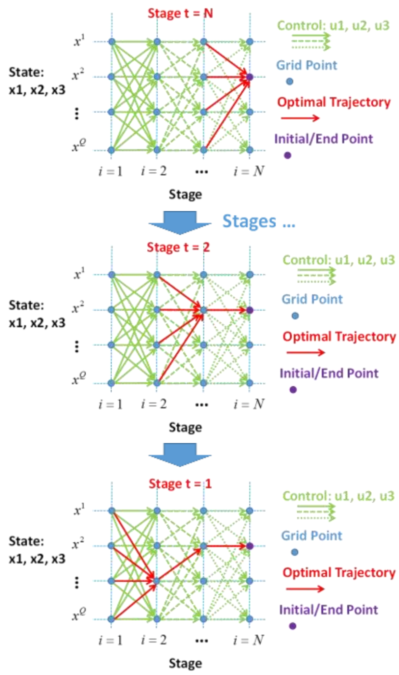

Fig. 8 DP Step 2: Backward Optimization

In this paper, DP is used to solve the relaxed optimization under different general drive cycles. Each time step of a drive cycle is considered as the stage of the control problem. Therefore, the problems are solved from the end of the drive cycle to the beginning.

5. OPTIMIZATION RESULTS AND ANALYSIS

Simulations results that compare non-relaxed and relaxed optimizations are conducted over 4 desired drive cycles: constant speed at 20mph, constant speed at 30mph, FUDS, and HWFET. The vehicle speed constraint is set to be ±2mph, and vehicle range is set to be ±5m. The optimized vehicle speed trajectories of the relaxed optimization for constant speed at 30mph and HWFET cycles are shown in Fig. 9. Pulse-and-glide behaviors of the vehicle speed are observed.

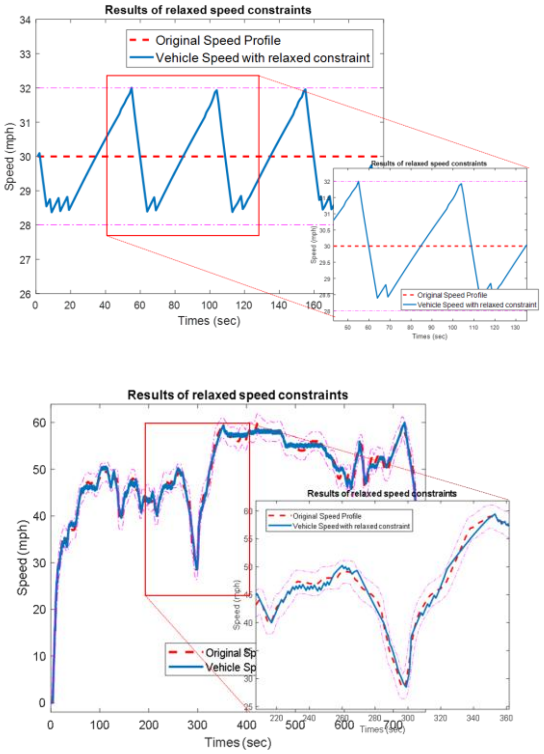

Fig. 9 Optimized Vehicle Speed of Relaxed Optimization at 30mph and HWFET

Fuel consumption results are summarized in Table 1. Results indicate that for the HEV, relaxing the vehicle speed and range constraints within the EPA defined tolerance can result in 3%-20% fuel reduction compared to the optimal results without relaxations.

Table 1 Summary of Fuel Consumption Results

Tested Cycles	Non-Relaxed (g)	Relaxed (g)	Fuel Reduction
Constant 20mph	171.89	142.32	17.2%
Constant 30mph	284.98	250.12	12.2%
FUDS	1538.9	1458.9	5.2%
HWFET	2144.3	2073.3	3.3%

Fig. 10 shows the fuel rates for relaxed optimization at the 30mph and 20mph cycles. The optimal engine power are mostly at around 23kW (near the "sweet spot" of the engine) or zero (engine shut-down). The resulted average fuel rates are lower than the fuel rate at the same average power level, as shown as the triangles. Therefore, the overall fuel consumption is reduced.

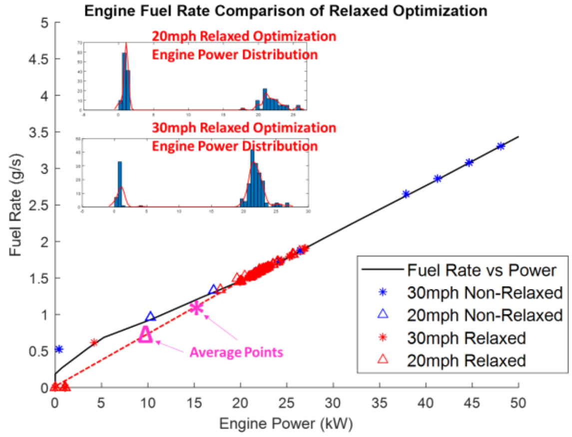

Fig. 10 Engine Fuel Rate for Relaxed Optimization

Relaxing the vehicle speed allow the vehicle to act as a (kinetic) energy storage system. An argument may be that the battery can replace the vehicle body to act as the energy buffer, which avoids speed fluctuation, and instead, the battery SOC will fluctuate up and down. This argument is less accurate due to the about 20% energy losses at motor and battery from our analysis. The optimal results show that this kinetic energy storage is preferred because it is more efficient than the battery system, due to its low energy conversion loss compared with the motor/battery system. The energy flow of the HEVs relaxed optimization is shown in Fig. 11.

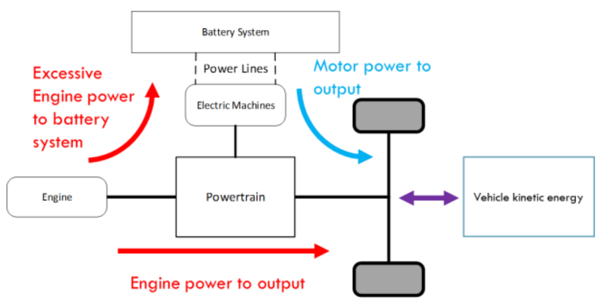

Fig. 11 6 Energy Flow of the Relaxed Optimization

The benefits of the relaxed optimization depends on other conditions, such as the defined speed constraint bounds, range constraint bounds, the drive cycle distribution, etc. To further analyze these problems for HEVs on general driving scenarios, more simulations are desirable. However, using DP to solve the problem is time consuming: taking over 9 days to complete the simulation on FUDS cycle. Using DP suffers the curse of dimensionality for the relaxed problems because of additional controls and states added. Different methods are desired to be exploited to solve these problems.

6. CONCLUSION

This paper studies the optimal control problem of HEVs with relaxed vehicle speed and range constraints.

Optimal results show the proposed speed-relaxed optimal control of HEVs reduces fuel consumption around 3%-20% under different test scenarios. Results also indicate that for the exemplary parallel HEV, it prefers vehicle speed pulse-and-glide over using electrical energy through battery to adjust engine operations, because the kinetic energy storage is more efficient than the battery system. Therefore, engine operates more around its sweet spot for the relaxed optimization for HEVs. Different methods are needed to further analyze these relaxed problems for HEVs on general driving scenarios.

REFERENCES

[1] "Fuel Economy Guide - Model Year 2018," United States Environmental Protection Agency. [Online]. Available: https://www.fueleconomy.gov/, 2018.

[2] R. L. Russell, K. Johnson, T. Durbin, P. P. Chen, J. Tomic, and R. Parish, "Emissions, fuel economy, and performance of a class 8 conventional and hybrid truck," SAE Technical Paper, doi: 2015-01-1083, 2015.

[3] Z. Pan, X. Zhang, E. Silvas, H. Peng, and N. Ravi, "Optimal design of all-wheel-drive hybrid pick-up trucks," in ASME 2015 Dynamic Systems and Control Conference, Columbus, 2015.

[4] E. Silvas, T. Hofman, A`. Serebrenik, and M. Steinbuch, "Functional and cost-based automatic generator for hybrid vehicles topologies," IEEE/ASME Transactions on Mechatronics, vol. 20, no. 4, pp. 1561-1572, 2015.

[5] X. Zhang, "Design of Power Split Hybrid Powertrains with Multiple Planetary Gears and Clutches," The University of Michigan, 2015.

[6] O. H. Dagci, "Hybrid Electric Powertrain Design and Control with Planetary Gear Sets for Performance and Fuel Economy," The University of Michigan, 2018.

[7] "Recommended Practice for Measuring the Exhaust Emissions and Fuel Economy of Hybrid-Electric Vehicles, Including Plug-in Hybrid Vehicles," SAE International, 2010.

[8] K. McDonough, I. Kolmanovsky, D. Filev, D. Yanakiev, S. Szwabowski, and J. Michelini, "Stochastic dynamic programming control policies for fuel efficient in-traffic driving." pp. 3986-3991.

[9] K. McDonough, I. Kolmanovsky, D. Filev, D. Yanakiev, S. Szwabowski, and J. Michelini, "Stochastic dynamic programming control policies for fuel efficient vehicle following." pp. 1350-1355.

[10] S. E. Li, H. Peng, K. Li, and J. Wang, "Minimum fuel control strategy in automated car-following scenarios," IEEE Transactions on Vehicular Technology, vol. 61, no. 3, pp. 998-1007, 2012.

[11] N. Mueller, S. Strauss, S. Tumback, G.-C. Goh, and A. Christ, "Next Generation Engine Start/Stop Systems:"Free-Wheeling"," SAE International Journal of Engines, vol. 4, no. 2011-01-0712, pp. 874-887, 2011.

[12] N. Müller, S. Strauss, S. Tumback, and A. Christ, "Coasting–Next Generation Start/Stop Systems," MTZ worldwide eMagazine, vol. 72, no. 9, pp. 14-19, 2011.

[13] S. E. Li, K. Deng, Y. Zheng, and H. Peng, "Effect of Pulse‐and‐Glide Strategy on Traffic Flow for a Platoon of Mixed Automated and Manually Driven Vehicles," Computer‐Aided Civil and Infrastructure Engineering, vol. 30, no. 11, pp. 892-905, 2015.

[14] S. Xu, S. E. Li, X. Zhang, B. Cheng, and H. Peng, "Fuel-optimal cruising strategy for road vehicles with step-gear mechanical transmission," IEEE Transactions on Intelligent Transportation Systems, vol. 16, no. 6, pp. 3496-3507, 2015.

[15] S. Xu, S. E. Li, H. Peng, B. Cheng, X. Zhang, and Z. Pan, "Fuel-Saving Cruising Strategies for Parallel HEVs," IEEE Transactions on Vehicular Technology, vol. 65, no. 6, pp. 4676-4686, 2016.

[16] R. Bellman, Dynamic programming: Courier Corporation, 2013.